Flashing lights affect the photophysiology and expression of carotenoid and lipid synthesis genes in *Nannochloropsis gaditana*

Serena Lima [a], Jep Lokesh [b,c], Peter S.C. Schulze [b,d], Rene H. Wijffels [b,e], Viswanath Kiron [b], Francesca Scargiali [a], Sebastian Petters [f], Hans C. Bernstein [f], Daniela Morales-Sánchez [b,f,*]

[a] *Engineering Department, University of Palermo, Italy*
[b] *Faculty of Biosciences and Aquaculture, Nord University, Bodø, Norway*
[c] *INRAE E2S UPPA, NUMEA, Université de Pau et des Pays de l'Adour, Saint-Pée-sur-Nivelle, France*
[d] *GreenColab – Associação Oceano Verde, University of Algarve, Faro, Portugal*
[e] *Bioprocess Engineering, AlgaePARC, Wageningen University, Netherlands*
[f] *The Norwegian College of Fisheries Sciences, Faculty of Biosciences, Fisheries and Economics, The Arctic University of Norway, Tromsø, Norway*

ARTICLE INFO

ABSTRACT

Nannochloropsis gaditana is a promising microalga for biotechnology. One of the strategies to stimulate its full potential in metabolite production is exposure to flashing lights. Here, we report how *N. gaditana* adapts to different flashing light regimes (5, 50, and 500 Hz) by changing its cellular physiology and the relative expression of genes related to critical cellular functions. We analyzed the differential mRNA abundance of genes related to photosynthesis, nitrogen assimilation and biosynthesis of chlorophyll, carotenoids, lipids, fatty acids and starch. Analysis of photosynthetic efficiency and high mRNA abundance of photoprotection genes supported the inference that excess excitation energy provided by light absorbance during photosynthesis was produced under low frequency flashing lights and was dissipated by photopigments via the xanthophyll-cycle. Increased relative expression levels of genes related to the synthesis of carotenoids and chlorophyll confirmed the accumulation of photopigments previously observed at low frequency flashing lights. Higher differential mRNA abundance of genes related to the triacylglycerol biosynthesis were observed at lower frequency flashing lights, possibly triggered by a poor nitrogen assimilation caused by low mRNA abundance of a nitrate reductase gene. This study advances a new understanding of algal physiology and metabolism leading to improved cellular performance and metabolite production.

1. Introduction

Photosynthetic microalgae have profound commercial applications mainly in human nutrition and in animal feed, especially in aquaculture, due to their high nutritional value (Matos, 2017). Research interests in microalgae are often based on enhancing production of high-value compounds such as carotenoids (Ambati et al., 2019), lipids (Xue et al., 2018), and especially polyunsaturated fatty acids (PUFAs) (Ramesh Kumar et al., 2019). In this context, the genus *Nannochloropsis* – an eustigmatophyte – has attracted a growing interest as an industrial strain due to relatively high yields of biomass and lipids (Rodolfi et al., 2009). The lipids of *Nannochloropsis* are mainly stored in the form of triacylglycerols (TAGs), which contain the ω-3 long-chain PUFA,

eicosapentaenoic acid (EPA) (Ma et al., 2016). Photopigments are another group of high-value compounds in the alga, including chlorophyll *a* and carotenoids, such as violaxanthin, vaucheraxanthin, zeaxanthin, and β-carotene (Rebolloso-Fuentes et al., 2001).

Different cultivation strategies have been investigated to control and optimize production of these bioproducts and other high-value biomolecules. The most commonly investigated approaches – for microalgae in general – has been to instigate an acute cellular stress response via nitrogen starvation, excessive light, or heat (Schüler et al., 2017; Yang et al., 2013). In comparison, the flashing light approach is an established tool for bioprocesses aiming to accumulate biomolecules (Katsuda et al., 2008, 2006; Kim et al., 2006; Takache et al., 2015) and/or to change the biochemical composition of microalgal biomass

(Matthijs et al., 1996). The 'flash' consists of illumination by dense packets of high-intensity actinic light spaced with controlled short periods of darkness instead of continuous exposure to the same average irradiance. The alternating frequency of light/dark (L/D) periods can be tuned to control and even optimize photosynthetic efficiency (Grobbelaar, 2010; Vejrazka et al., 2013). An advantage of FL is that it can be used to avoid photoinhibition caused by excess excitation under continuous light (CL) by relaxing the light harvesting complex during the L/D cycle. Optimization of an FL regime for a given cultivation process can therefore result in algal cells that more efficiently utilize light energy (Abu-Ghosh et al., 2015; Béchet et al., 2013). In addition, FL also promotes a relatively enhanced dark reactions' rate which may lead to photosynthesis enhancement – i.e*.,* more efficient electron transfer rate (ETR) between photosystem I (PSI) and photosystem II (PSII) than under CL (where ETR is about ten times slower than the rate of light capture by chlorophyll) (Abu-Ghosh et al., 2016).

Several possible physiological mechanisms for the FL effect have been described, including: 1) photoacclimation, 2) post-illumination enhanced respiration, 3) photodynamic damage to the 32 kDa protein of PSII, 4) activation of the xanthophyll cycle, and 5) thermal-energy dissipation (Abu-Ghosh et al., 2016; Iluz et al., 2012). This established "flashing light effect" indicates that both the frequency and magnitude of actinic light can alter intracellular molecules that can cause changes in the physiology of the cell. Hence, the study of the expression of key genes involved in photosynthesis and photopigments and lipid biosynthesis could be a useful tool to understand the cellular processes in the adaptation to different flashing light regimes. This strategy has been previously deployed as a useful tool to investigate a known subset of *N. gaditana* genes that are responsive to environmental stressors including nitrogen starvation (Liang et al., 2019). In our earlier work, we analyzed the growth efficiency and productivity, as well as the biochemical composition of *N. gaditana* under three different frequencies of flashing light (5 Hz, 50 Hz and 500 Hz) compared to continuous light (Lima et al., 2021). Here, we go further to report a targeted gene expression profile of microalgal biomass obtained in these previous experiments along with the analysis of photosynthetic efficiency. These new results enable inference of how *N. gaditana* adapts to changing flashing light regimes and may therefore help guide future strategies aimed at creating new control approaches to increase content of high-value biomolecular compounds in microalgal biomass.

2. Materials and methods

2.1. Strain and culture conditions

The marine microalga *Nannochloropsis gaditana* CCAP 849/5 was obtained from the Scottish Association for Marine Science (Oban, Scotland) and cultivated at 20 °C. The algal stock was maintained on agar plates containing modified f/2 medium (Guillard and Ryther, 1962). The inoculant was developed in 500 mL shake-flasks (100 rpm) containing 100 mL of modified f/2 medium. All media were prepared with filtered seawater from the North Atlantic coast of Bodø (Norway), which has a salinity of about 35, and was combined with components of the f/2 medium consisting of 5.3 mM $NaNO_3$, 0.22 mM $NaH_2PO_4 \cdot H_2O$, 35 µM $FeCl_3 \cdot 6H_2O$, 35 µM $Na_2EDTA \cdot 2H_2O$, 0.12 µM $CuSO_4 \cdot 5H_2O$, 0.078 µM $Na_2MoO_4 \cdot 2H_2O$, 0.23 µM $ZnSO_4 \cdot 7H_2O$, 0.126 µM $CoCl_2 \cdot 6H_2O$, 2.73 µM $MnCl_2 \cdot 4H_2O$, 8.88 µM thiamine HCl, 0.06 µM biotin and 0.012 µM cyanocobalamin with a pH of 7.2.

2.2. Flashing light set-up

Cultivation for all flashing light experiments were performed using batch cultivation for 13 days in tissue culture flasks (Falcon Scientific, Seaton Delaval, UK) with a total working volume of 250 mL (light path: 3.7 cm). Humidified and filtered air (0.2 µm, Acrodisc ® PTFE filter, Pall Corporation, USA) enriched in 1 % (v/v) CO_2 was supplied to each cultivation unit at a flow rate of 160 mL min^{-1} using a rotameter (Omega, Manchester, UK) for controlling CO_2 supply and mixing.

The mounting of light source and the application of the flashing light conditions were as described in our previous publication (Lima et al., 2021). The flashing light conditions applied were: continuous light (CL) and flashing light (FL) with a duty cycle of 0.05 with frequencies of 5 (FL5), 50 (FL50), and 500 (FL500) Hz. The time-averaged light intensity was I_a = 300 µmol s^{-1} m^{-2} under all conditions, which corresponded to an instantaneous flash intensity of I_l = 6000 µmol s^{-1} m^{-2}. Under FL5, the light period (t_l) was 10 ms and the dark period (t_d) was 190 ms; under FL 50 t_l was 1 ms and t_d was 10 ms and under FL500, the t_l was 0.1 and t_d was 0.19 ms. The flashes were set using PWM-OCX (RMCybernetics Ltd, Alsager, UK) pulse width modulators (PWMs) powered by a bench power supply EA-PS 2084–05B (EA Elektro-Automatik). The pulse signal was provided by a TG4001 (TTi, Huntingdon, UK) function generator or directly by the PWMs. LEDs were also connected directly to the power supply units for continuous light control treatments. The LEDs were regulated to adjust I_a to 300 µmol s^{-1} m^{-2} and compensate switching and working losses at the LEDs and PWMs. The supplied light intensity (i.e., photosynthetically active radiation) was measured for one minute at the same position as the flasks (SPQA 5234 connected to a data logger LI-1500, Li-Cor, Lincoln, NE, USA) and averaged over time.

2.3. Growth measurement

Daily samples of the culture (0.5–1 mL) were taken to measure absorbance at 540 nm in a 1 cm microcuvette using a spectrophotometer (Hach-Lange DR3900, Hach, International, CO, USA). Dry cell weight (DCW) was determined gravimetrically by filtering 5–10 mL of the culture through a pre-dried and weighed glass fiber membrane filter (Millipore, MA, USA) with a 0.45 µm pore size. A calibration curve between absorbance measured at 750 nm (A750) and DCW was constructed ($W = 0.884 \cdot A_{750} + 0.0117$, $R^2 = 0.99$) for the daily calculation of biomass concentration (W).

2.4. Photosynthetic efficiency

The photosynthetic performance of the cultures was measured by chlorophyll *a* fluorescence using a pulse-amplitude modulated (PAM) fluorometer (Diving-PAM, Walz GmbH, Effeltrich, Germany). For measurements, algal samples from cultures were adjusted to 1.0 g DW L^{-1} with seawater (salinity 35), and 1.2 mL was transferred to a 3 mL glass cuvette (1.0 cm light path, VWR, Oslo, Norway) and mixed with a magnetic stirrer. The minimum (F_0) and maximum fluorescence (F_m) yields were measured after 1 h dark incubation, and used to calculate maximum PSII-quantum yields (F_v/F_m). A saturation pulse was then applied (> 9000 µmol s^{-1}m^{-2}, 0.6 s) and effective PSII-quantum yields were measured using the minimum (F) and maximum fluorescence (F_m') yields of algal samples exposed to a series of gradually increasing actinic light intensities (41–1452 µmol s^{-1}m^{-2}). The test light intensities were provided every 10 s. Finally, the effective PSII quantum yields (F_v'/F_m') were obtained. Relative photosynthetic electron transport rates (ETRs) were calculated by multiplying the effective PSII-quantum yields by the incident actinic light intensities. These data were plotted against the incident actinic light intensities and fitted using the Jassby and Platt equation (Jassby and Platt, 1976) to estimate the maximum ETRs (ETRmax), the light saturation points of photosynthesis (E_k), and the initial slopes of the ETR vs. irradiance curves (α_{ETR}).

2.5. RNA extraction

Total cell RNA was extracted from cultures of *N. gaditana* at a concentration of 1×10^6 cells/mL using the E.Z.N.A® total DNA/RNA isolation kit (Omega Bio-tek, Inc., GA, USA). The *N. gaditana* samples taken from different flashing light treatments were centrifuged at 2000 x g, 4 °C for 5 min, the supernatant was discarded, and the pellet was

stored at $-80\ °C$ for at least 24 h. After this time, 700 μL of lysis buffer from the E.Z.N.A® total DNA/RNA isolation kit was added to the sample prior to disrupting cells using a bead mill (Bertin technologies, Precellys Evolution, Montigny-le-Bretonneux, France) with a mixture of 0.1 mm glass beads and 1.4 mm ceramic beads. Samples were centrifuged at $10,000{\times}g$, $4\ °C$ for 10 min. The supernatant was used for RNA isolation according to manufacturer's protocol.

2.6. cDNA synthesis

Reverse transcription reactions were performed using SuperScript™ IV VILO™ Master Mix with the enzyme ezDNase (Invitrogen™, ThermoFisher Scientific, MA, USA) according to the manufacturer's protocol. Briefly, a total amount of 1.4 μg of RNA from *N. gaditana* was treated with ezDNase enzyme (SuperScript™ IV VILO™ Master Mix with ezD-Nase enzyme, ThermoFisher Scientific) to remove any contaminating DNA. The synthesized cDNA, diluted 1:10 with deionized water (Invitrogen™ Nuclease-Free Water, ThermoFisher Scientific), was then used as a template in quantitative PCR reactions.

2.7. RT-qPCR reactions

Primers were designed using the PearlPrimer (Marshall, 2004). Sequence data corresponding to the specific targets were retrieved from the database (http://www.nannochloropsis.org/). Primers were designed to flank and overlap the intron-exon boundary to make them specific to the transcripts and avoid binding to genomic DNA. The qPCR reactions were performed by mixing 5 μL of FastStart Universal SYBR Green Master mix (Rox) (Roche Molecular Systems, Inc., CA, USA) with 1 μL of primer mix (consisting of forward and the reverse primers) at a concentration of 300 nM and 4 μL of the cDNA. The conditions of thermocycling were: $95\ °C$ for 600 s (preincubation), followed by 40 cycles of denaturation at $95\ °C$ for 10 s, annealing/extension at $60\ °C$ for 30 s (LightCycler 96, Roche Molecular Systems, Inc.). A melting curve analysis was performed for each sample to check the specificity of the primers. Target gene data were normalized using the normalization factor calculated based on the expression of the 2 most stable reference genes (housekeeping genes) phosphatidic acid phosphatase (*PAP1*) and cyclophilin (*CYP*). Fig. S3 shows the relative gene expression of all the reference genes used in this study under the control (CL) and flashing light (FL) conditions. All calculations were performed using geNorm (Vandesompele et al., 2002). The list of primers and the accession numbers are shown in the Supplemental Table S2. The fold change was calculated dividing the normalized relative expression of the sample (FL) between the normalized relative expression of the control (CL). Therefore, the fold change value of the control (CL) is always 1 for each gene.

2.8. Statistical analysis

The Saphiro-Wilk test was used to verify the normal distribution of the data and the Brown-Forsythe test was applied to confirm the homogeneity of variance between treatments. One-way analysis of variance (ANOVA) and *post-hoc* Tukey's multiple comparison test were applied to each set of experiments to determine statistical differences between treatments. *P* values less than 0.05 were considered statistically significant. The fold changes between the CL condition and the FL conditions were obtained from the mRNA abundance level of the FL conditions divided by the mRNA abundance level of the CL condition. Therefore, the value of the relative fold change for the CL condition was always 1, and the abundance level changes up or down in the FL conditions. A *t*-student test with a *p* value of < 0.05 was applied to each set of normalized values in order to determine statistical differences in abundance levels. RT-PCR data is available in GEO NCBI GSE210188 (https://www.ncbi.nlm.nih.gov/geo/query/acc.cgi?acc=GSE210188). Photosynthetic physiology data, calculations and figure generation

scripts are provided and linked to R markdown files deposited in GitHub project: spe238/nanno_gene_expr (https://github.com/spe238/nanno_gene_expr).

3. Results and discussion

3.1. Nannochloropsis gaditana physiology is responsive to FL

N. gaditana responds to different flashing light regimes by varying its growth rate and total biomass yields (Fig. 1a). It reached its highest biomass concentrations and growth rates under the continuous light treatment (CL) and the highest frequency of light pulses (FL500) tested (4.16 ± 0.22 g L^{-1} and 0.414 ± 0.02 days^{-1} and 3.8 ± 0.49 g L^{-1} and 0.35 ± 0.03 days^{-1}; $p > 0.05$, respectively). Lower biomass concentrations and a longer lag phase were observed when *N. gaditana* cells were exposed to FL5 and FL50 (0.18 ± 0.01 and 1.72 ± 0.17 g L^{-1}, respectively; $p < 0.05$) as compared to the FL500 and CL conditions. This result is contextualized from our previous reported results (Lima et al., 2021), where we determined that proteins, PUFA, chlorophyll and violaxanthin, among other intracellular compounds which are normally thought to accumulate under low-light conditions, were induced under low frequency flashing light (FL5 and FL50). However, typical high-light biomolecules such as lutein and *β*-carotene were also partially increased under low-frequency flashing light.

Cells grown in FL5 and FL50 had higher photosynthetic efficiency than the other two conditions analyzed (FL500 and CL; Fig. 1b and Table S1). This analysis of fluorescence-based photophysiology (Table S1) indicated that although the maximum quantum yield of PSII was the same in all conditions (α-parameter), the effective quantum yield (Fv'/Fm') was highest when cells were treated to FL50. Furthermore, the maximum photosynthetic capacity (ETR$_{max}$) was higher in FL50 and FL5 treatments and there was no measurable difference in terms of the theoretical light saturation (E$_k$) between FL regimes.

It is tempting to suggest that when *N. gaditana* cultures were irradiated with low frequency FL, a significant decoupling of energy flux from the enhanced photosynthetic process and carbon metabolism was observed.

This is supported by the fact that though growth rates and biomass concentrations were lower at FL5 and FL50 higher photosynthetic efficiencies were observed, contrary to what happened at higher FL. Hence, the excess of energy excitation provided by photosynthesis was dissipated as heat by photopigments via the xanthophyll-cycle, a phenomenon that takes place during short-term photoacclimation (Demmig-Adams and Adams, 1996). At the lower frequency FL conditions, the photoinhibition may have been reduced since the light exposure was too short to cause damage and/or the periodic dark intervals facilitated the *de novo* repair of the damage (Abu-Ghosh et al., 2016; Iluz et al., 2012). One possible explanation for the lower photosynthetic efficiency obtained at high FL frequency conditions is that the respiration rate was probably lower for the light signals, thus resulting in less energy consumption, leading to an optimum photosynthetic process supporting growth (Abu-Ghosh et al., 2016). In addition, at this high frequency FL conditions the amount of ATP generated in the electron transfer chain was sufficient to support the comparably slow Calvin cycle throughout the dark phase and allowed for its continuous operation yielding higher growth rates (Abu-Ghosh et al., 2016; Falkowski and Raven, 2007).

3.2. Low frequency FL dissipates excess energy through the violaxanthin cycle

Violaxanthin de-epoxidase (VDE) and zeaxanthin epoxidase (ZE) are involved in a photoprotection mechanism in one of the xanthophyll cycles, the violaxanthin cycle (Fig. 2), which protects cells from the oxidative stress that occurs under high-light stress (Latowski et al., 2011). The differential transcript abundance of *VDE-2* (Figs. 2 and 3a)
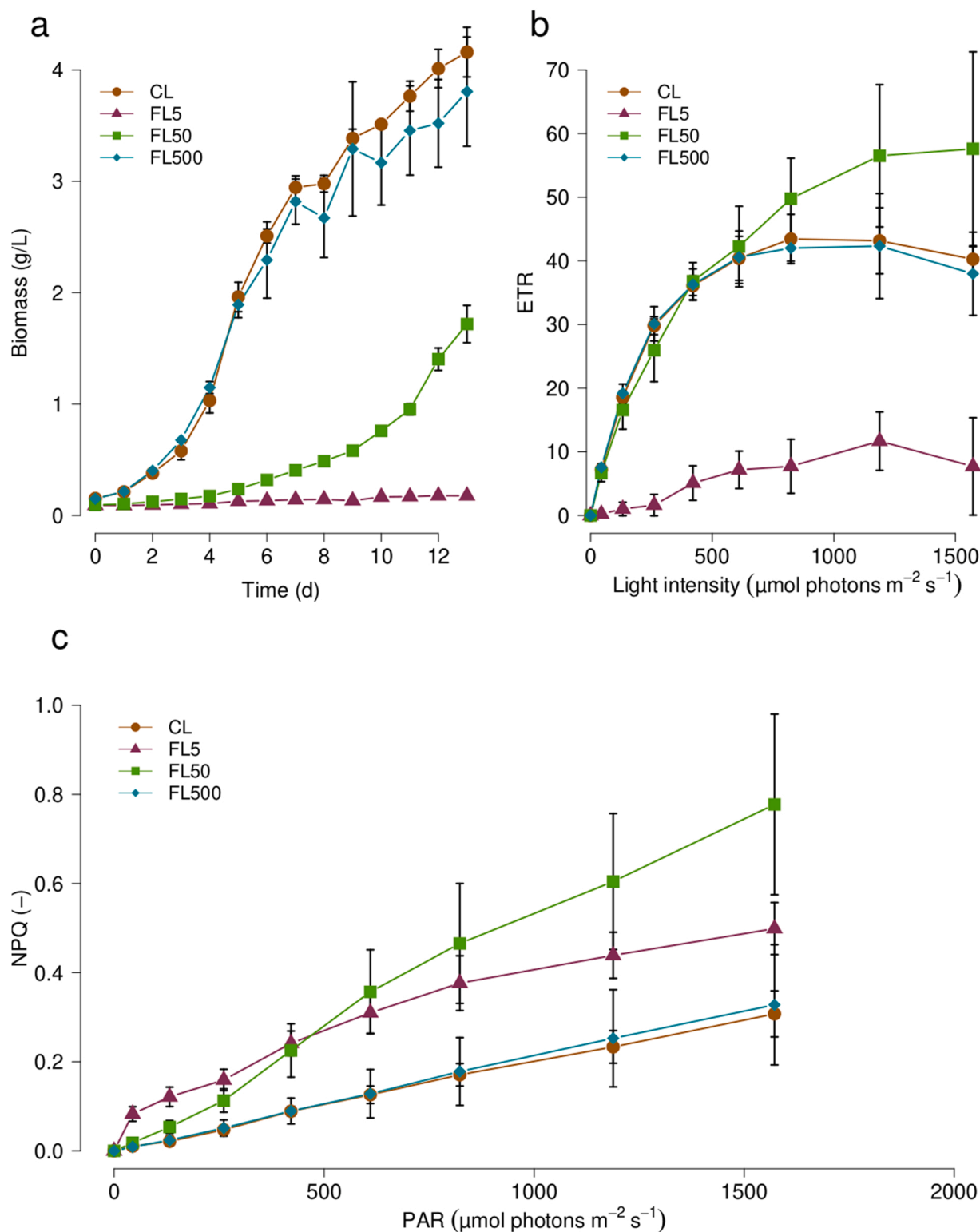
Fig. 1. The effect of flashing light (FL5, FL50, and FL500) and continuous light (CL) on growth (a), photosynthetic irradiance (P-I) (b) and non-photochemical quenching (NPQ) (c) instigate different growth and photosynthetic physiologies in batch cultures of *N. gaditana*. Cells were cultured under continuous light or flashing light with duty cycle of 0.05 and frequencies of 5, 50, 500 Hz at an average light intensity of I_a= 300 μmol s^{-1} m^{-2}. Data points with error bars on each day are expressed as mean ± SD (n = 3).

was significantly higher in FL5 compared to the CL (2.4-fold; $p < 0.0001$), while the other treatments did not show any significant differences from CL. VDE catalyzes the de-epoxidation of violaxanthin to yield zeaxanthin at saturating light intensities (Fig. 2) (Jahns et al., 2009). The highly abundance of the *VDE* genes ensures that zeaxanthin

accumulates at saturating light intensity (Jahns et al., 2009) that may be present in FL5. But, this should be highly regulated since high amounts of zeaxanthin can inhibit the activity of VDE through a feedback mechanism (Hieber et al., 2004). In addition, at FL5 we previously found high amounts of violaxanthin (Lima et al., 2021), which is controlled by
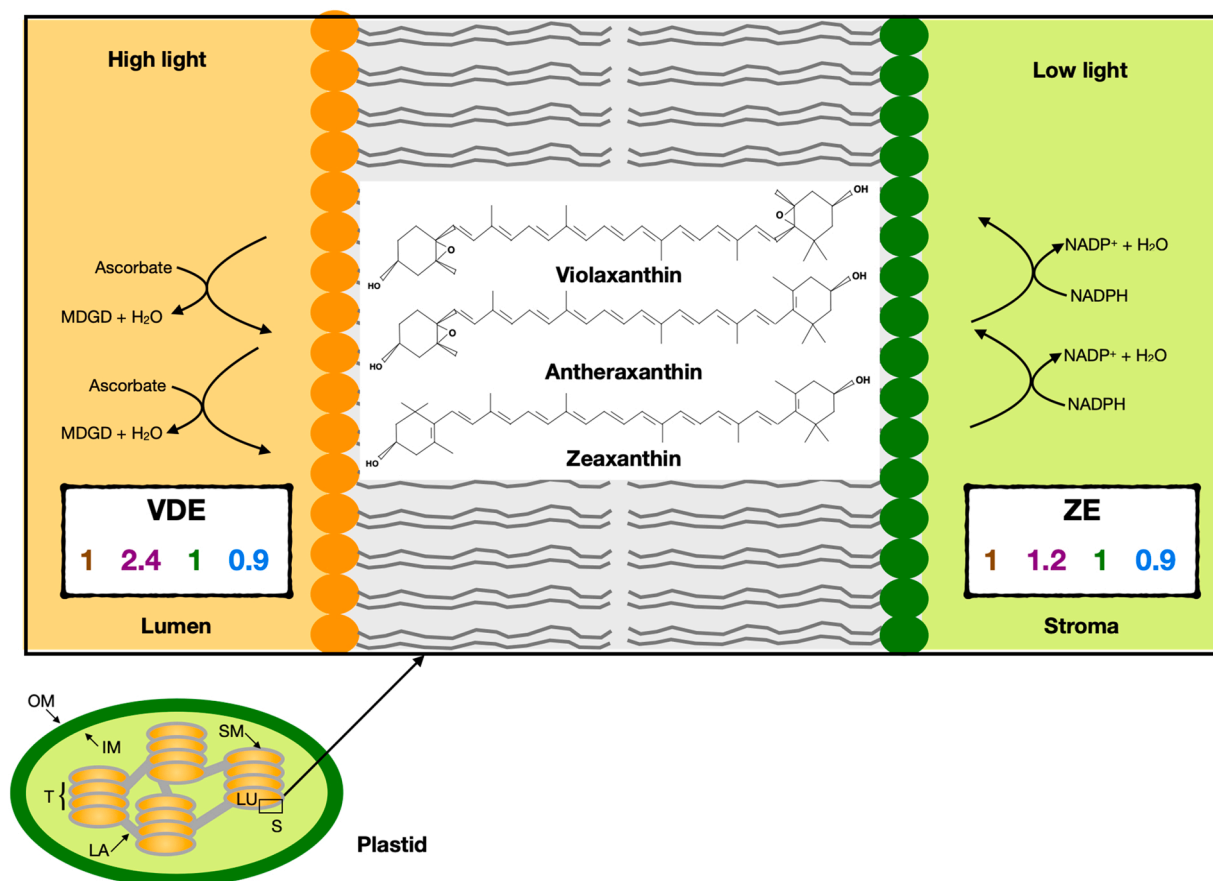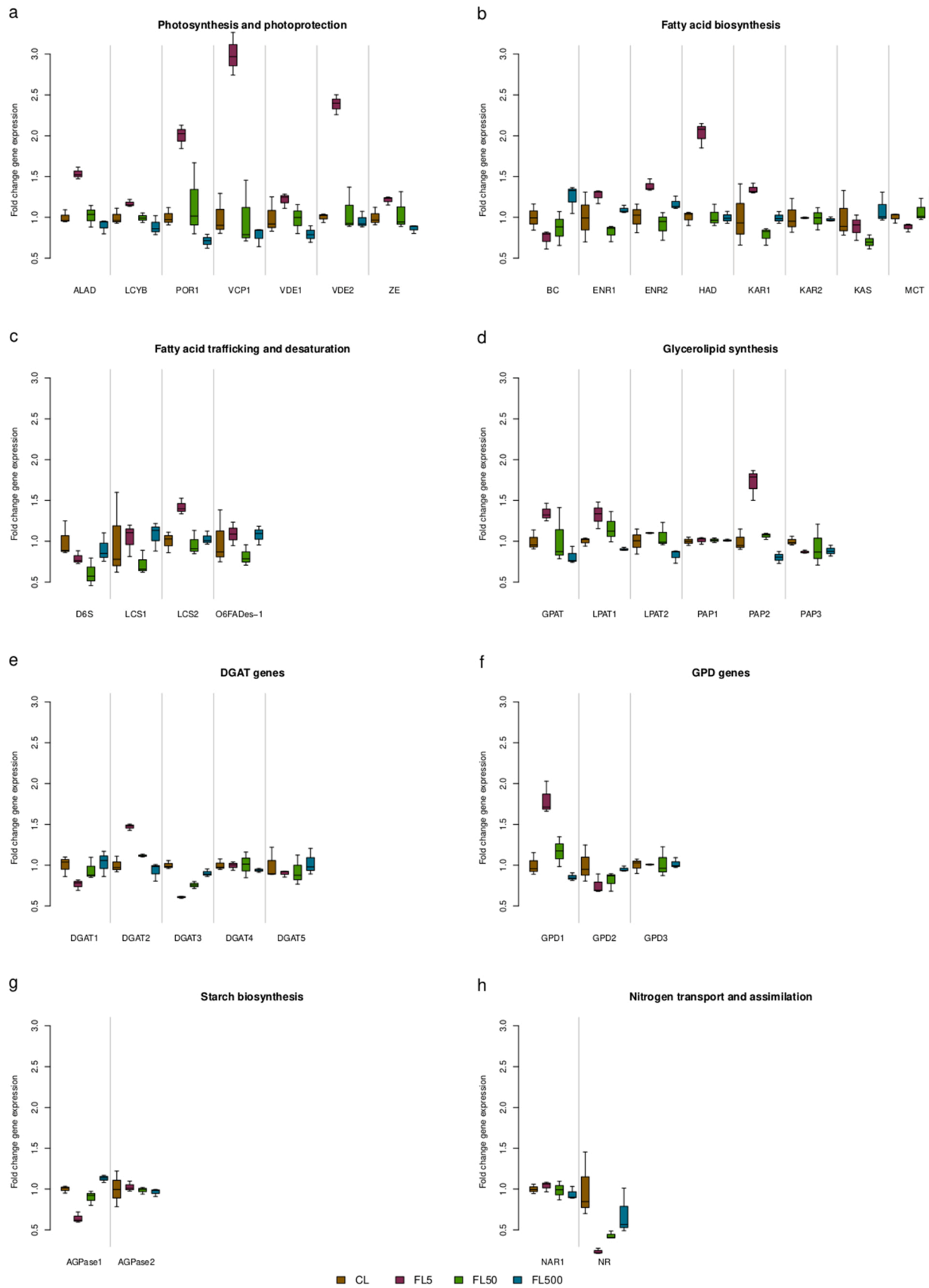
Fig. 2. Low frequency FL dissipates excess energy through the violaxanthin cycle. *Nannochloropsis gaditana* was cultured under continuous light or flashing light with duty cycle of 0.05 and frequencies of 5, 50, 500 Hz at an average light intensity of $I_a = 300$ µmol s^{-1} m^{-2}. The numbers in the white box represent the fold-changes in the transcript abundance (mean of three independent experiments, two tailed Student's *t*-test, $p < 0.05$). Numbers in brown, purple, green and sky blue represent the CL, FL5, FL50 and FL500 treatments, respectively. IM: inner membrane; LA: lamella; LU: lumen; M: stroma membrane; OM: Outer membrane; S: stroma; S T: thylakoids; *VDE*: violaxanthin de-epoxidase; *ZE*: zeaxanthin epoxidase.

the expression of the *VDE* gene (Arvidsson et al., 1996), whose expression level vary in response to changes in the VAZ (violaxanthin, antheraxanthin, zeaxanthin) pool size (Bugos et al., 1999).

Though we did not measure zeaxanthin in our previous studies, we suggest measurements of this metabolite in future research because this pigment plays a central role in different photoprotective mechanisms in chloroplasts. The pigment acts as antioxidant in the lipid phase of the thylakoid membrane of the protein/lipid interphase (Havaux et al., 2007; Havaux and Niyogi, 1999; Johnson et al., 2007), and contributes essentially to the dissipation of excess excitation energy (non-photochemical quenching, NPQ) in the antenna of PSII (Demmig et al., 1987; Niyogi et al., 1998, 1997). In this context, measurements of NPQ (Fig. 1c) showed that FL5 had higher energy dissipation levels than CL, confirming an essential role of the violaxanthin cycle for energy dissipation at low frequency FL.

On the other hand, the transcript abundance of *ZE* does not show significant differences between CL and all the treatments (Fig. 3a; $p > 0.05$), which may indicate that the expression level of this gene is regulated at the post-transcriptional level or the activity of this gene product may be constitutive (Jahns et al., 2009). In addition, the expression of *ZE* was found to be constant during day/night-cycle experiments in several higher plants (Audran et al., 1998; North et al., 2005; Wang et al., 2008). The product of the gene *ZE* catalyzes the epoxidation of zeaxanthin to become violaxanthin at low light intensities (Jahns et al., 2009). The *VCP* gene encoding the violaxanthin–chlorophyll a binding protein is the major protein in the light harvesting complex (LHC) of *N. gaditana*. It binds chlorophyll a and the

carotenoids violaxanthin and vaucheriaxanthin and is involved in triplet–triplet energy transfer, which occurs between chlorophyll and carotenoid molecules to dissipate energy under light stress conditions (Carbonera et al., 2014; Keşan et al., 2016; Litvín et al., 2016). The transcript abundance of this gene was 3-times higher at the lowest frequency FL condition (FL5; Fig. 3a); than the control and the other treatments ($p < 0.01$), indicating a strong light stress, which may be caused by the high light energy ($I_I = 6000$ µmol m^{-2} s^{-1}) for the light flash period (t_I) of 10 ms, compared to the 1 and 0.1 ms of the FL50 and FL500 conditions, respectively, and the continuous light (CL). VCP has a fundamental role in photoprotection (Carbonera et al., 2014); the present results correlates with our previous findings on adaptation to both high and low light in algae grown under FL5 (Lima et al., 2021). Lycopene β cyclase (LCYB) encodes for a key enzyme in the biosynthetic pathway of isoprenoids, specifically catalyzing the formation of the bi-cyclic β-carotene from the linear, symmetric lycopene (Cunningham and Gantt, 1998; Olmos-soto and Ruiz, 2012). Fig. 3a and Supplementary 1a show the transcript abundance of this gene, which was higher in FL5 compared to FL500 ($p < 0.05$) but similar to CL and FL50 ($p > 0.05$). Despite the similarities of the abundance of this gene under low frequency FL and CL conditions, we found previously that the synthesis of carotenoids was promoted under low frequency FL (Lima et al., 2021). However, the accumulation of carotenoids cannot be directly linked to adaptation to low or high light, as some carotenoids are associated with a protective function against oxidation caused by high light (Varela et al., 2015), while some others are associated with adaptation to low light (Schüler et al., 2017). Either way, the presence of

a Photosynthesis and photoprotection

b Fatty acid biosynthesis

c Fatty acid trafficking and desaturation

d Glycerolipid synthesis

e DGAT genes

f GPD genes

g Starch biosynthesis

h Nitrogen transport and assimilation

CL   FL5   FL50   FL500

(caption on next page)

Fig. 3. Differential mRNA abundance (fold change) of genes related to photosynthesis and photoprotection (a), fatty acid biosynthesis (b), fatty acid trafficking and desaturation (c), glycerolipid synthesis (d), *DGAT* genes (e), *GPD* genes (f), starch biosynthesis (g), nitrogen transport and assimilation (h). Cells of *N. gaditana* were cultured under continuous light (CL) and under different flashing light frequencies (5 Hz: FL5; 50 Hz: FL50, and 500 Hz: FL500). FL5, FL50 and FL500 treatments are compared with the CL condition (control), therefore the fold-change varies up or down with respect to the CL treatment that was always 1. Relative gene expression for all genes are shown in Fig. S1. *AGPase*: ADP-glucose pyrophosphorylase, *ALAD*: alanine dehydratase, *BC*: biotin carboxylase, *DGAT*: Diacylglycerol O-acyl-transferase, *ENR*: enoyl-ACP reductase, *GPAT*: acylCoA:glycerol-3-phosphate acyltransferase, *GPD*: Glycerol 3-phosphate dehydrogenase, *HAD*: hydroxyacyl-ACP dehydratase, *KAR*: the ketoacyl-ACP reductase, *KAS*: 3-ketoacyl-ACP synthase, *LCS*: long-chain acyl-CoA synthetase, *LCYB*: lycopene β cyclase, *LPAT*: acyl-CoA: lysophosphatidic acyltransferase, *MCT*: malonyl-CoA transacylase, *NAR*: nitrate transporter, *NR*: nitrate reductase, *O6FADes*: Δ6-desaturase, *PAP*: phosphatidic acid phosphatase, *POR*: protochlorophyllide oxidoreductase, *VCP*: violaxanthin–chlorophyll a binding protein, *VDE*: violaxanthin de-epoxidase, *ZE*: zeax-anthin epoxidase.

carotenoids (Lima et al., 2021) and the increased differential mRNA abundance of *LCYB* strongly suggest cellular photoprotective and adaptive mechanisms under continuous light and low frequency FL.

The alanine dehydratase (ALAD) and protochlorophyllide oxidore-ductase (POR) enzymes are involved in the tetrapyrrole and chlorophyll synthesis (Tanaka and Tanaka, 2007). The differential mRNA abundance of the respective genes coding for these enzymes increased in FL5 compared to CL ($p < 0.01$) and to the other treatments ($p < 0.05$), corresponding to the accumulation of chlorophyll as previously observed under FL5 (Lima et al., 2021).

3.3. Low frequency FL produce low total lipid content but increases the expression level of genes involved in the Kennedy pathway suggesting some level of stress

N. gaditana is an industrially relevant species due to its relatively high yield of lipids (Rodolfi et al., 2009). Therefore, we investigated the effect of flashing light on the expression of genes related to lipid synthesis, particularly those involved in the *de novo* fatty acid biosynthesis (Fig. 3b).

Values on the Y-axis indicate the mean and standard deviation of three independent experiments. Samples indicated with an asterisk are significantly different from the control ($p < 0.05$) in a two tailed Student's *t*-test.

The gene *BC*, in Fig. 3b and S1b, encodes biotin carboxylase (BC), an enzyme that is part of the heteromeric form of acetyl-CoA carboxylase (ACCase), located in the chloroplast of *Nannochloropsis* and is responsible for the first step of *de novo* fatty acid synthesis. BC carboxylates acetyl-CoA to generate malonyl-CoA, a molecule that after being activated with an acyl carrier protein (ACP; Fig. S2) enters into the fatty acid synthetase complex to form fatty acids (Fig. 4) (Li-Beisson et al., 2019; Mühlroth et al., 2013). The differential mRNA abundance of *BC* was 1.7-times lower in FL5 than in FL500 (Fig. 3b; $p < 0.05$), but similar to CL ($p > 0.05$). Nevertheless, this may suggest that less CO_2 is carboxylated to malonyl-CoA in FL5 compared to FL500. As a result, lipid biosynthesis (based on total lipid content) might be comparatively reduced under low FL (FL5), as has been previously observed [12].

The gene *MCT*, also shown in Fig. 3b and S1b, encodes malonyl-CoA transacylase (MCT), which converts malonyl-CoA to malonyl-ACP (Li-Beisson et al., 2019). The differential transcript abundance level of this gene was similar between CL and all treatments (Fig. 3b, $p > 0.05$). The other analyzed genes shown in Fig. 3b encode enzymes that constitute the Fatty Acid Synthase (FAS) complex: 3-ketoacyl-ACP synthase (KAS), hydroxyacyl-ACP dehydratase (HAD), ketoacyl-ACP reductase (KAR) and enoyl-ACP reductase (ENR) (Li-Beisson et al., 2013). The complex ligates Malonyl-ACP to an acetyl-CoA molecule to form a 3-ketoacyl-ACP by the action of KAS, while releasing one molecule of CO_2. The 4-carbon 3-ketoacyl-ACP is then reduced by KAR to

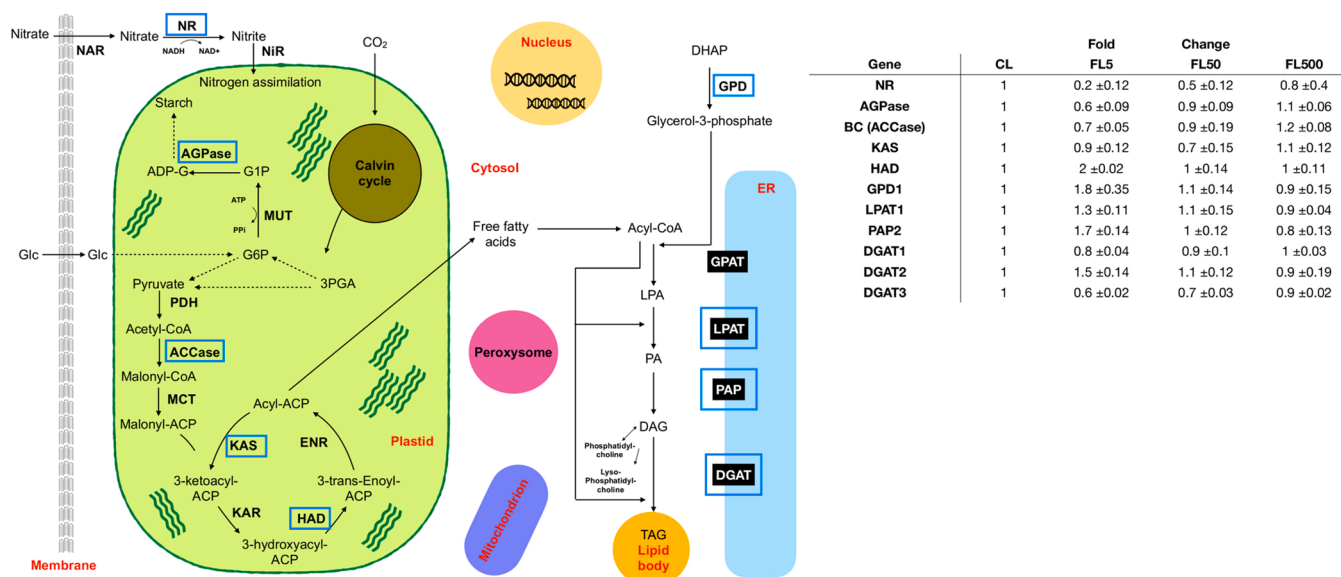| Gene	CL	Fold Change		
		FL5	FL50	FL500
NR	1	0.2 ±0.12	0.5 ±0.12	0.8 ±0.4
AGPase	1	0.6 ±0.09	0.9 ±0.09	1.1 ±0.06
BC (ACCase)	1	0.7 ±0.05	0.9 ±0.19	1.2 ±0.08
KAS	1	0.9 ±0.12	0.7 ±0.15	1.1 ±0.12
HAD	1	2 ±0.02	1 ±0.14	1 ±0.11
GPD1	1	1.8 ±0.35	1.1 ±0.14	0.9 ±0.15
LPAT1	1	1.3 ±0.11	1.1 ±0.15	0.9 ±0.04
PAP2	1	1.7 ±0.14	1 ±0.12	0.8 ±0.13
DGAT1	1	0.8 ±0.04	0.9 ±0.1	1 ±0.03
DGAT2	1	1.5 ±0.14	1.1 ±0.12	0.9 ±0.19
DGAT3	1	0.6 ±0.02	0.7 ±0.03	0.9 ±0.02

Fig. 4. Low frequency FL increases the expression level of genes involved in the Kennedy pathway. Cells of *N. gaditana* were cultured under continuous light (CL) and under different flashing light frequencies (5 Hz: FL5; 50 Hz: FL50, and 500 Hz: FL500). FL5, FL50 and FL500 treatments are compared with the CL condition (control), therefore the fold-change varies up or down with respect to the CL treatment that was always 1. Genes highlighted in a blue box presented significant differences in fold changes in at least one condition when compared to the control (two tailed Student's *t*-test, $p < 0.05$). 3PGA: 3-phosphoglycerate; ACCase: acyl-CoA carboxylase; ACP: acyl carrier protein; ADP-G: adenosine diphosphate glucose; AGPase: glucose-1-phosphate adenylyltransferase; CoA: coenzyme A; DAG: diacylglycerol; DGAT: diacylglycerol acyltransferase; ENR: enoyl-ACP reductase; G1P: glucose-1-phosphate; G6P: glucose-6-phosphate; GPAT: glycerol-3-phosphate acyltransferase; GPD: glycerol-3-phosphate dehydrogenase; HAD: β-hydroxyacyl-ACP dehydrase; KAR: β-ketoacyl-ACP reductase; KAS: β-ketoacyl-ACP synthase; LPA: lysophosphatidic acid; LPAT: 1-acyl-sn-glycerol-3-phosphate acyltransferase; MCT: malonyl-CoA transacylase; MUT: mutase; NAR: nitrate transporter; NiR: nitrite reductase; NR: nitrate reductase; PA: phosphatidic acid; PAP: phosphatidic acid phosphatase; PDH: pyruvate dehydrogenase; TAG: triacylglycerol.

3-hydroxyacyl-ACP, dehydrated by HAD to 3-trans-enoyl-ACP, and again reduced by ENR to acyl-ACP to finally yield a 6-carbon-ACP molecule (Fig. 4; [37]). Among these genes, only *HAD* showed increased differential mRNA abundance level in FL5 as compared to CL (2-times higher, $p < 0.0001$, Fig. 3b) and to the other treatments ($p < 0.05$). Despite differential abundance of this gene and the low lipid content observed under FL5, transcript abundances of the other genes involved in FAS remained constant regardless of the FL regime.

The expression levels of genes involved in fatty acid trafficking and desaturation are shown in Fig. 3c. Two genes of the long-chain acyl-CoA synthetase protein were found in the *N. gaditana* genome database (*LCS1* and *LCS2*). Of them, only *LCS2* had higher differential mRNA abundance level in FL5 compared to CL (Fig. 3c, $p < 0.01$) and to the other treatments ($p < 0.05$). *LCS* family genes have been shown to be involved in lipid movement between the endoplasmic reticulum and plastid in *Arabidopsis* (Jessen et al., 2015). They activate non-esterified fatty acids to their CoA esters after release from a membrane lipid or TAG. Although they have been identified in algae, the putative orthologues of this family and their functions in fatty acid export have not yet been studied (Li-Beisson et al., 2019), making it difficult to put forth an explanation for the different expression levels of *LCS1* and *2*. The high differential mRNA abundance level of *LCS2* suggests that some trafficking of "old" fatty acids (not *de novo*) occurred under low frequency flashing light conditions, however, this is not a conclusive observation.

The expression level of the gene Δ6-desaturase (*O6FADes*) was similar in all treatments as compared to CL ($p > 0.05$; Fig. 3c). The product of this gene catalyzes the production of a double bond in both α-linoleic and linolenic acids (Khozin-Goldberg et al., 2002; Ma et al., 2011; Wiktorowska-Owczarek et al., 2015) and is therefore critical in the synthesis of PUFAs. However, this result is not sufficient to explain the accumulation of PUFAs previously observed in FL5 and FL50 (Lima et al., 2021). Therefore, it could be a different level of regulation, for instance, the upregulation of another desaturase downstream in the biosynthesis pathway, for example the stearoyl-ACP desaturase (Li-Beisson et al., 2019) or the *ω*-3 fatty acid desaturase (Sato et al., 2017). It could also be regulated during the elongation process through a cytosolic type I FAS, that regulates the elongation of >C18 fatty acids (Li-Beisson et al., 2019).

Responsive genes show that the Kennedy pathway is affected by variable FL regimes. Glycerolipids (Fig. 3d) are synthesized by an ensemble of reactions known as the Kennedy pathway (Cagliari et al., 2011; Li-Beisson et al., 2019, 2015). This pathway (Fig. 4) involves the enzymes acylCoA:glycerol-3-phosphate acyltransferase (GPAT), acyl-CoA:lysophosphatidic acyltransferase (LPAT), diacylglycerol acyltransferase (DGAT), and phosphatidic acid phosphatase (PAP). The metabolic pathway begins with the acylation of glycerol-3-phosphate (G3P) by GPAT. Phosphatidic acid (PA) is then formed in another acyl-CoA-dependent acylation catalyzed by LPAT. PAP catalyzes the release of a phosphate molecule to form diacylglycerol (DAG). The final step is the acylation of DAG to produce TAG, which is controlled by DGAT (Cagliari et al., 2011). The differential mRNA abundance level of *GPAT* was similar in all treatments as compared to CL ($p > 0.05$). Between *LPAT1* and *2* only the first one showed significant differences, being higher in FL5 compared to CL ($p > 0.01$). Similar observations were made under a different stress condition (Li et al., 2014). When *Nannochloropsis* was kept under nitrogen deprivation, only a few *LPAT* genes showed different expression levels, suggesting that the isoforms of the gene individually respond to the stress to which the cells are exposed (Li et al., 2014). As for the *PAP* genes, there were statistical differences only in *PAP2* and *3*. *PAP2* showed higher differential mRNA abundance level in FL5 than in the CL ($p < 0.01$), while *PAP3* had it slightly lower in FL5 than in the CL ($p < 0.05$). Similarly, in *Chlamydomonas reinhardtii*, among the different isoforms of PAP only one is correlated with lipid accumulation (Deng et al., 2013).

With respect to the three *DGAT* genes (Fig. 3e) there were statistical differences: *DGAT1* and *3* had lower differential transcript abundance

levels in FL5 than in the CL ($p < 0.05$ and $p < 0.001$, respectively) while *DGAT2* presented higher differential mRNA abundance level in FL5 as compared to CL ($p < 0.01$). Genes *DGAT4* and *5* had the same transcript abundance levels under the different light conditions when compared to CL ($p > 0.05$). In *C. reinhardtii* there are six DGATs isoforms of two types, type 1 DGAT and five type 2 DGTT (Li-Beisson et al., 2019). This high number of *DGAT* genes in *Chlamydomonas* is still not clear but it is speculated to be due to different acyl-CoA specificities (substrate preference), or to different subcellular locations, or to the need for DGAT isoforms adapted to specific effectors of enzyme activity that may be produced under the various TAG-inducing stress (Li-Beisson et al., 2015). The differential mRNA abundance level of *N. gaditana DGAT2* is opposite to that of *DGAT1* and *DGAT3*. As noted for *C. reinhardtii* DGATs, it is likely that *N. gaditana* DGATs have distinct functions in lipid metabolism, responding also to the environmental conditions.

The GPD genes were also responsive to low frequency FL conditions. However, statistical differences are observed only for *GPD1* (Fig. 3f), whose differential mRNA abundance level was higher in FL5 than in the CL and the other conditions ($p < 0.05$). The enzyme GPD catalyzes the formation of the glycerol backbone for the assembly of TAG (Morales-Sánchez et al., 2017). The abundance of this gene transcript could possibly be associated to an increase in the G3P pool for TAG synthesis. However, as TAG content was not quantified here or in our previous study (Lima et al., 2021); therefore this connection will have to be investigated in future studies. The *GPD2* and *3* genes have constant mRNA abundance levels. In *C. reinhardtii*, it has been demonstrated that all GPD isoforms have distinct functions that are highly dependent on environmental conditions (Goodenough et al., 2014; Morales-Sánchez et al., 2017). *GPD2* in *C. reinhardtii* was upregulated under nitrogen starvation, while *GPD3* was stimulated when cells grow at high osmolarity. It is very likely that the GPD isoforms of *N. gaditana*, as in the case of *C. reinhardtii*, also have different functions that enable them to adapt to the environmental conditions. Thus, though only *GPD1* responded to the flashing light conditions, specifically to the low frequency FL, it is possible that the other isoforms might respond to nutrient or salt stress.

Overall, the differential transcript abundance of the genes related to the synthesis of TAG tended to increase in low than in high frequency FL and continuous light. This indicates that more TAGs are present in cells grown under these conditions, even though the previous experimental results showed lower total lipid content (~40 % lower) under lower frequency than at higher frequency FL and CL [12]. However, in our previous study, only the total lipid amount was analyzed under the different conditions, and not the TAG content. This could lead to the inference that although a decrease in total lipids was observed under the low frequency flashing light conditions, the lipids could mainly be present as TAG, pointing to some level of stress caused by this type of light.

3.4. Low frequency FL causes low expression of an AGPase gene without compromising total starch production, while negatively affecting the nitrogen assimilation in cell, causing poor growth performance

The differential transcript abundance level of ADP-glucose pyrophosphorylase 1 (*AGPase1*) is significantly lower in FL 5 compared to CL and to the other treatments ($p < 0.01$), while *AGPase2* has no significant difference in mRNA abundance levels ($p > 0.05$) between the CL and the treatments (Fig. 3g). The ADP-glucose pyrophosphorylase gene is essential for starch synthesis and catalyzes the reaction of one molecule of glucose-1-phosphate with one molecule of ATP to form one molecule of ADP-glucose and one molecule of pyrophosphate (Fig. 4) (Ho et al., 2014). In our previous studies (Lima et al., 2021), it was shown that the intracellular starch content was similar under all conditions. Therefore, the differential expression of *AGPase-1* might be related to another function rather than starch synthesis.

In turn, the differential mRNA abundance level of the gene *NAR1* (Fig. 3h) was similar under all light conditions ($p > 0.05$), including the

CL. *NAR1* encodes Nitrate Assimilation-Related component 1 and has the function of a nitrate transporter (Fig. 4) (Sanz-Luque et al., 2015). Similar levels of transcript abundance suggest that there is no difference in nitrite recruitment under different lighting conditions. Nitrate reductase (NR) is responsible for the first step of nitrogen assimilation and reduces nitrate to nitrite (Fig. 4) (Kilian et al., 2011). The differential mRNA abundance level of *NR* was lower in FL5 compared to the CL (Fig. 3h; $p < 0.05$). Deficient nitrogen assimilation could be indicative of the poor growth performance under this condition. The transcript abundance level of this gene at lower frequency FL and its effects on lipid synthesis are unclear, but we suggest that it may be responsible for the suspected TAG synthesis under these stress conditions. In other algal species, including *Nannochloropsis*, nitrogen limitation can trigger TAG accumulation (Schüler et al., 2017; Yang et al., 2013). This may also explain why the transcript abundance of some of the genes in the Kennedy pathway were increased, specifically *LPAT1* (1.3-fold), *PAP-2* (1.7-fold), and *DGAT* (1.5-fold), even from GPD (1.8-fold), to provide the glycerol backbone for TAG assembly. In support of this theory, the mRNA abundance level of the gene coding for the major biosynthetic enzyme for starch biosynthesis AGPase was decreased (0.64-fold) possibly to direct the carbon flux to the TAG synthesis. However, we are unable to substantiate this statement as we have not examined the contribution of TAG to total lipids in our studies.

4. Conclusion

Our results shed light on the complexity of the metabolic responses of *N. gaditana* to different flashing light conditions. Higher photosynthetic efficiency was found under low frequency flashing light conditions (FL5 and FL50). This excess of energy excitation was not directed to cell growth but dissipated as heat by photopigments via the xanthophyll-cycle. To support this, the transcript abundance level of the violaxanthin de-epoxidase gene and other photoprotection genes were substantially higher at low frequency FL. Furthermore, the mRNA abundance levels of some genes related to the lipid biosynthetic and the Kennedy pathways were higher at the lowest frequency FL (FL5), though it was not reflected in the total lipid content. Nevertheless, we hypothesize that the high transcript abundance of the Kennedy pathway genes leads to a presumable accumulation of TAG molecules and are also responsible for the higher PUFA content observed previously at low frequency flashing light. It is likely that the alga was subjected to nitrogen stress at low frequency FL as the nitrate reductase gene had low mRNA abundance levels which also could triggers TAG synthesis. Our observations will enable researchers to elucidate new molecular strategies to engineer the production of photopigments and other high-value biomolecular compounds in *N. gaditana* biomass.

CRediT authorship contribution statement

Serena Lima: Writing – original draft, Methodology. **Jep Lokesh:** Methodology, Writing – original draft. **Peter S.C. Schulze:** Methodology, Writing – original draft. **Rene H. Wijffels:** Writing – original draft. **Viswanath Kiron:** Writing – original draft. **Francesca Scargiali:** Writing – original draft. **Sebastian Petters:** Writing – original draft. **Hans C. Bernstein:** Writing – original draft. **Daniela Morales-Sánchez:** Methodology, Writing – original draft.

Declaration of Competing Interest

The authors declare the following financial interests/personal relationships which may be considered as potential competing interests: Rene Wijffels reports financial support was provided by Research Council of Norway.

Data Availability

I have shared the link to my data/code at the attach file step.

Appendix A. Supporting information

Supplementary data associated with this article can be found in the online version at doi:10.1016/j.jbiotec.2022.11.012.

References

Abu-Ghosh, S., Fixler, D., Dubinsky, Z., Solovchenko, A., Zigman, M., Yehoshua, Y., Iluz, D., 2015. Flashing light enhancement of photosynthesis and growth occurs when photochemistry and photoprotection are balanced in Dunaliella salina. Eur. J. Phycol. 50, 469–480. https://doi.org/10.1080/09670262.2015.1069404/SUPPL_FILE/TEJP_A_1069404_SM5257.TIF.

Abu-Ghosh, S., Fixler, D., Dubinsky, Z., Iluz, D., 2016. Flashing light in microalgae biotechnology. Bioresour. Technol. 203, 357–363. https://doi.org/10.1016/J.BIORTECH.2015.12.057.

Ambati, R.R., Gogisetty, D., Aswathanarayana, R.G., Ravi, S., Bikkina, P.N., Bo, L., Yuepeng, S., 2019. Industrial potential of carotenoid pigments from microalgae: current trends and future prospects. Crit. Rev. Food Sci. Nutr. 59, 1880–1902. https://doi.org/10.1080/10408398.2018.1432561.

Arvidsson, P.O., Bratt, C.E., Carlsson, M., Åkerlund, H.E., 1996. Purification and identification of the violaxanthin deepoxidase as a 43 kDa protein. Photosynth. Res. 492 (49), 119–129. https://doi.org/10.1007/BF00117662.

Audran, C., Borel, C., Frey, A., Sotta, B., Meyer, C., Simonneau, T., Marion-Poll, A., 1998. Expression studies of the zeaxanthin epoxidase gene in Nicotiana plumbaginifolia. Plant Physiol. 118, 1021. https://doi.org/10.1104/PP.118.3.1021.

Béchet, Q., Shilton, A., Guieysse, B., 2013. Modeling the effects of light and temperature on algae growth: state of the art and critical assessment for productivity prediction during outdoor cultivation. Biotechnol. Adv. 31, 1648–1663. https://doi.org/10.1016/J.BIOTECHADV.2013.08.014.

Bugos, R.C., Chang, S.H., Yamamoto, H.Y., 1999. Developmental expression of violaxanthin de-epoxidase in leaves of tobacco growing under high and low light. Plant Physiol. 121, 207–213. https://doi.org/10.1104/PP.121.1.207.

Cagliari, A., Margis, R., Dos Santos Maraschin, F., Turchetto-Zolet, A.C., Loss, G., Margis-Pinheiro, M., 2011. Biosynthesis of Triacylglycerols (TAGs) in plants and algae. Int. J. Plant Biol. 2, 10. https://doi.org/10.4081/pb.2011.e10.

Carbonera, D., Agostini, A., Di Valentin, M., Gerotto, C., Basso, S., Giacometti, G.M., Morosinotto, T., 2014. Photoprotective sites in the violaxanthin–chlorophyll a binding Protein (VCP) from Nannochloropsis gaditana. Biochim. Biophys. Acta - Bioenerg. 1837, 1235–1246. https://doi.org/10.1016/j.bbabio.2014.03.014.

Cunningham, F.X., Gantt, E., 1998. Genes and enzymes of carotenoid biosynthesis in plants. Annu. Rev. Plant Physiol. Plant Mol. Biol. 49, 557–583. https://doi.org/10.1146/annurev.arplant.49.1.557.

Demmig, B., Winter, K., Krüger, A., Czygan, F.-C., 1987. Photoinhibition and zeaxanthin formation in intact leaves: a possible role of the xanthophyll cycle in the dissipation of excess light energy. Plant Physiol. 84, 218–224. https://doi.org/10.1104/PP.84.2.218.

Demmig-Adams, B., Adams, W.W., 1996. The role of xanthophyll cycle carotenoids in the protection of photosynthesis. Trends Plant Sci. 1, 21–26. https://doi.org/10.1016/S1360-1385(96)80019-7.

Deng, X., Cai, J., Fei, X., 2013. Involvement of phosphatidate phosphatase in the biosynthesis of triacylglycerols in Chlamydomonas reinhardtii. J. Zhejiang Univ. Sci. B 14, 1121–1131. https://doi.org/10.1631/jzus.B1300180.

Falkowski, P.G., Raven, J.A., 2007. Aquatic Photosynthesis, 2nd edition.,. Princet. Univ. Press, p. 484.

Goodenough, U., Blaby, I., Casero, D., Gallaher, S.D., Goodson, C., Johnson, S., Lee, J.H., Merchant, S.S., Pellegrini, M., Roth, R., Rusch, J., Singh, M., Umen, J.G., Weiss, T.L., Wulan, T., 2014. The path to triacylglyceride obesity in the sta6 strain of Chlamydomonas reinhardtii. Eukaryot. Cell 13, 591–613. https://doi.org/10.1128/EC.00013-14.

Grobbelaar, J.U., 2010. Microalgal biomass production: challenges and realities. Photosynth. Res. 106, 135–144. https://doi.org/10.1007/S11120-010-9573-5.

Guillard, R.R., Ryther, J.H., 1962. Studies of marine planktonic diatoms. I. Cyclotella nana Hustedt, and Detonula confervacea (cleve) Gran. Can. J. Microbiol. https://doi.org/10.1139/m62-029.

Havaux, M., Niyogi, K.K., 1999. The violaxanthin cycle protects plants from photooxidative damage by more than one mechanism. Proc. Natl. Acad. Sci. USA 96, 8762–8767. https://doi.org/10.1073/PNAS.96.15.8762.

Havaux, M., Dall'Osto, L., Bassi, R., 2007. Zeaxanthin has enhanced antioxidant capacity with respect to all other xanthophylls in arabidopsis leaves and functions independent of binding to PSII antennae. Plant Physiol. 145, 1506–1520. https://doi.org/10.1104/PP.107.108480.

Hieber, A.D., Kawabata, O., Yamamoto, H.Y., 2004. Significance of the lipid phase in the dynamics and functions of the xanthophyll cycle as revealed by PsbS overexpression in tobacco and in-vitro de-epoxidation in Monogalactosyldiacylglycerol micelles. Plant Cell Physiol. 45, 92–102. https://doi.org/10.1093/PCP/PCH010.

Ho, S.-H., Ye, X., Hasunuma, T., Chang, J.-S., Kondo, A., 2014. Perspectives on engineering strategies for improving biofuel production from microalgae — a critical review. Biotechnol. Adv. 32, 1448–1459. https://doi.org/10.1016/J.BIOTECHADV.2014.09.002.

Iluz, D., Alexandrovich1, I., Dubinsky, Z., 2012. The enhancement of photosynthesis by fluctuating light. Artif. Photosynth. https://doi.org/10.5772/31040.

Jahns, P., Latowski, D., Strzalka, K., 2009. Mechanism and regulation of the violaxanthin cycle: The role of antenna proteins and membrane lipids. Biochim. Biophys. Acta - Bioenerg. 1787, 3–14. https://doi.org/10.1016/J.BBABIO.2008.09.013.

Jassby, A.D., Platt, T., 1976. Mathematical formulation of the relationship between photosynthesis and light for phytoplankton. Limnol. Oceanogr. https://doi.org/10.4319/lo.1976.21.4.0540.

Jessen, D., Roth, C., Wiermer, M., Fulda, M., 2015. Two activities of long-chain acyl-coenzyme a synthetase are involved in lipid trafficking between the endoplasmic reticulum and the plastid in arabidopsis. Plant Physiol. 167, 351–366. https://doi.org/10.1104/pp.114.250365.

Johnson, M.P., Havaux, M., Triantaphylidès, C., Ksas, B., Pascal, A.A., Robert, B., Davison, P.A., Ruban, A.V., Horton, P., 2007. Elevated zeaxanthin bound to oligomeric LHCII enhances the resistance of arabidopsis to photooxidative stress by a lipid-protective, Antioxidant Mechanism. J. Biol. Chem. 282, 22605–22618. https://doi.org/10.1074/JBC.M702831200.

Katsuda, T., Shimahara, K., Shiraishi, H., Yamagami, K., Ranjbar, R., Katoh, S., 2006. Effect of flashing light from blue light emitting diodes on cell growth and astaxanthin production of Haematococcus pluvialis. J. Biosci. Bioeng. 102, 442–446. https://doi.org/10.1263/JBB.102.442.

Katsuda, T., Shiraishi, H., Ishizu, N., Ranjbar, R., Katoh, S., 2008. Effect of light intensity and frequency of flashing light from blue light emitting diodes on astaxanthin production by Haematococcus pluvialis. J. Biosci. Bioeng. 105, 216–220. https://doi.org/10.1263/JBB.105.216.

Keşan, G., Litvín, R., Bína, D., Durchan, M., Šlouf, V., Polívka, T., 2016. Efficient light-harvesting using non-carbonyl carotenoids: energy transfer dynamics in the VCP complex from Nannochloropsis oceanica. Biochim. Biophys. Acta - Bioenerg. 1857, 370–379. https://doi.org/10.1016/j.bbabio.2015.12.011.

Khozin-Goldberg, I., Didi-Cohen, S., Shayakhmetova, I., Cohen, Z., 2002. Biosynthesis of eicosapentaenoic acid (EPA) in the freshwater Eustigmatophyte Monodus subterraneus (Eustigmatophyceae). J. Phycol. 38, 745–756. https://doi.org/10.1046/j.1529-8817.2002.02006.x.

Kilian, O., Benemann, C.S.E., Niyogi, K.K., Vick, B., 2011. High-efficiency homologous recombination in the oil-producing alga Nannochloropsis sp. Proc. Natl. Acad. Sci. USA 108, 21265–21269. https://doi.org/10.1073/pnas.1105861108.

Kim, Z.-H.H., Kim, S.-H.H., Lee, H.-S.S., Lee, C.-G.G., 2006. Enhanced production of astaxanthin by flashing light using Haematococcus pluvialis. Enzym. Microb. Technol. 39, 414–419. https://doi.org/10.1016/J.ENZMICTEC.2005.11.041.

Latowski, D., Kuczyńska, P., Strzałka, K., 2011. Xanthophyll cycle – a mechanism protecting plants against oxidative stress. Redox Rep. 16, 78–90. https://doi.org/10.1179/174329211×13020951739938.

Li, J., Han, D., Wang, D., Ning, K., Jia, J., Wei, L., Jing, X., Huang, S., Chen, J., Li, Y., Hu, Q., Xu, J., 2014. Choreography of Transcriptomes and Lipidomes of Nannochloropsis Reveals the Mechanisms of Oil Synthesis in Microalgae. Plant Cell 26, 1645–1665. https://doi.org/10.1105/tpc.113.121418.

Liang, J., Wen, F., Liu, J., 2019. Transcriptomic and lipidomic analysis of an EPA-containing Nannochloropsis sp. PJ12 in response to nitrogen deprivation. Sci. Rep. 9 https://doi.org/10.1038/s41598-019-41169-2.

Li-Beisson, Y., Shorrosh, B., Beisson, F., Andersson, M.X., Arondel, V., Bates, P.D., Baud, S., Bird, D., DeBono, A., Durrett, T.P., Franke, R.B., Graham, I.A., Katayama, K., Kelly, A.A., Larson, T., Markham, J.E., Miquel, M., Molina, I., Nishida, I., Rowland, O., Samuels, L., Schmid, K.M., Wada, H., Welti, R., Xu, C., Zallot, R., Ohlrogge, J., 2013. Acyl-Lipid Metabolism. Arab. Book. BioOne, e0161. https://doi.org/10.1199/table0161.

Li-Beisson, Y., Beisson, F., Riekhof, W., 2015. Metabolism of acyl-lipids in Chlamydomonas reinhardtii. Plant J. 82, 504–522. https://doi.org/10.1111/tpj.12787.

Li-Beisson, Y., Thelen, J.J., Fedosejevs, E., Harwood, J.L., 2019. The lipid biochemistry of eukaryotic algae. Prog. Lipid Res. 74, 31–68. https://doi.org/10.1016/j.plipres.2019.01.003.

Lima, S., Schulze, P.S.C., Schüler, L.M., Rautenberger, R., Morales-Sánchez, D., Santos, T.F., Pereira, H., Varela, J.C.S., Scargiali, F., Wijffels, R.H., Kiron, V., 2021. Flashing light emitting diodes (LEDs) induce proteins, polyunsaturated fatty acids and pigments in three microalgae. J. Biotechnol. https://doi.org/10.1016/j.jbiotec.2020.11.019.

Litvín, R., Bína, D., Herbstová, M., Gardian, Z., 2016. Architecture of the light-harvesting apparatus of the eustigmatophyte alga Nannochloropsis oceanica. Photosynth. Res. 130, 137–150. https://doi.org/10.1007/s11120-016-0234-1.

Ma, X., Yu, J., Zhu, B., Pan, K., Pan, J., Yang, G., 2011. Cloning and characterization of a delta-6 desaturase encoding gene from Nannochloropsis oculata. Chin. J. Oceanol. Limnol. 29, 290–296. https://doi.org/10.1007/s00343-011-0048-0.

Ma, X.-N., Chen, T.-P., Yang, B., Liu, J., Chen, F., 2016. Lipid production from nannochloropsis. Mar. Drugs 14, 61. https://doi.org/10.3390/md14040061.

Marshall, O.J., 2004. PerlPrimer: cross-platform, graphical primer design for standard, bisulphite and real-time PCR. Bioinformatics 20, 2471–2472. https://doi.org/10.1093/bioinformatics/bth254.

Matos, Â.P., 2017. The impact of microalgae in food science and technology. JAOCS J. Am. Oil Chem. Soc. https://doi.org/10.1007/s11746-017-3050-7.

Matthijs, H.C.P., Balke, H., Van Hes, U.M., Kroon, B.M.A., Mur, L.R., Binot, R.A., 1996. Application of light-emitting diodes in bioreactors: flashing light effects and energy economy in algal culture (Chlorella pyrenoidosa). Biotechnol. Bioeng. 50, 98–107. https://doi.org/10.1002/(SICI)1097-0290(19960405)50:1<98::AID-BIT11>3.0.CO;2-3.

Morales-Sánchez, D., Kim, Y., Terng, E.L., Peterson, L., Cerutti, H., 2017. A multidomain enzyme, with glycerol-3-phosphate dehydrogenase and phosphatase activities, is involved in a chloroplastic pathway for glycerol synthesis in Chlamydomonas reinhardtii. Plant J. 90, 1079–1092. https://doi.org/10.1111/tpj.13530.

Mühlroth, A., Li, K., Røkke, G., Winge, P., Olsen, Y., Hohmann-Marriott, M., Vadstein, O., Bones, A., 2013. Pathways of lipid metabolism in marine algae, co-expression network, bottlenecks and candidate genes for enhanced production of EPA and DHA in species of chromista. Mar. Drugs 11, 4662–4697. https://doi.org/10.3390/md11114662.

Niyogi, K.K., Björkman, O., Grossman, A.R., 1997. Chlamydomonas xanthophyll cycle mutants identified by video imaging of chlorophyll fluorescence quenching. Plant Cell 9, 1369–1380. https://doi.org/10.1105/TPC.9.8.1369.

Niyogi, K.K., Grossman, A.R., Björkman, O., 1998. Arabidopsis mutants define a central role for the xanthophyll cycle in the regulation of photosynthetic energy conversion. Plant Cell 10, 1121–1134. https://doi.org/10.1105/TPC.10.7.1121.

North, H.M., Frey, A., Boutin, J.P., Sotta, B., Marion-Poll, A., 2005. Analysis of xanthophyll cycle gene expression during the adaptation of Arabidopsis to excess light and drought stress: Changes in RNA steady-state levels do not contribute to short-term responses. Plant Sci. 169, 115–124. https://doi.org/10.1016/J.PLANTSCI.2005.03.002.

Olmos-soto, J., Ruiz, M.A., 2012. Microbial Carotenoids from Bacteria and Microalgae. https://doi.org/10.1007/978-1-61779-879-5.

Ramesh Kumar, B., Deviram, G., Mathimani, T., Duc, P.A., Pugazhendhi, A., 2019. Microalgae as rich source of polyunsaturated fatty acids. Biocatal. Agric. Biotechnol. 17, 583–588. https://doi.org/10.1016/j.bcab.2019.01.017.

Rebolloso-Fuentes, M.M., Navarro-Pérez, A., García-Camacho, F., Ramos-Miras, J.J., Guil-Guerrero, J.L., 2001. Biomass nutrient profiles of the microalga nannochloropsis. J. Agric. Food Chem. 49, 2966–2972. https://doi.org/10.1021/jf0010376.

Rodolfi, L., Zittelli, G.C., Bassi, N., Padovani, G., Biondi, N., Bonini, G., Tredici, M.R., 2009. Microalgae for oil: Strain selection, induction of lipid synthesis and outdoor mass cultivation in a low-cost photobioreactor. Biotechnol. Bioeng. 102, 100–112. https://doi.org/10.1002/bit.22033.

Sanz-Luque, E., Chamizo-Ampudia, A., Llamas, A., Galvan, A., Fernandez, E., 2015. Understanding nitrate assimilation and its regulation in microalgae. Front. Plant Sci. 6 https://doi.org/10.3389/fpls.2015.00899.

Sato, N., Moriyama, T., Mori, N., Toyoshima, M., 2017. Lipid metabolism and potentials of biofuel and high added-value oil production in red algae. World J. Microbiol. Biotechnol. 33 https://doi.org/10.1007/S11274-017-2236-3.

Schüler, L.M., Schulze, P.S.C., Pereira, H., Barreira, L., León, R., Varela, J., 2017. Trends and strategies to enhance triacylglycerols and high-value compounds in microalgae. Algal Res. 25, 263–273. https://doi.org/10.1016/j.algal.2017.05.025.

Takache, H., Pruvost, J., Marec, H., 2015. Investigation of light/dark cycles effects on the photosynthetic growth of Chlamydomonas reinhardtii in conditions representative of photobioreactor cultivation. Algal Res. 8, 192–204. https://doi.org/10.1016/j.algal.2015.02.009.

Tanaka, R., Tanaka, A., 2007. Tetrapyrrole biosynthesis in higher plants. Annu. Rev. Plant Biol. 58, 321–346. https://doi.org/10.1146/annurev.arplant.57.032905.105448.

Vandesompele, J., De Preter, K., Pattyn, F., Poppe, B., Van Roy, N., De Paepe, A., Speleman, F., 2002. Accurate normalization of real-time quantitative RT-PCR data by geometric averaging of multiple internal control genes. Genome Biol. 3 https://doi.org/10.1186/gb-2002-3-7-research0034.

Varela, J.C., Pereira, H., Vila, M., León, R., 2015. Production of carotenoids by microalgae: achievements and challenges. Photosynth. Res. 125, 423–436. https://doi.org/10.1007/s11120-015-0149-2.

Vejrazka, C., Janssen, M., Benvenuti, G., Streefland, M., Wijffels, R.H., 2013. Photosynthetic efficiency and oxygen evolution of Chlamydomonas reinhardtii under continuous and flashing light. Appl. Microbiol. Biotechnol. 97, 1523–1532. https://doi.org/10.1007/S00253-012-4390-8.

Wang, N., Fang, W., Han, H., Sui, N., Li, B., Meng, Q.W., 2008. Overexpression of zeaxanthin epoxidase gene enhances the sensitivity of tomato PSII photoinhibition to high light and chilling stress. Physiol. Plant. 132, 384–396. https://doi.org/10.1111/J.1399-3054.2007.01016.X.

Wiktorowska-Owczarek, A., Berezińska, M., Nowak, J., 2015. PUFAs: structures, metabolism and functions. Adv. Clin. Exp. Med. 24, 931–941. https://doi.org/10.17219/acem/31243.

Xue, Z., Wan, F., Yu, W., Liu, J., Zhang, Z., Kou, X., 2018. Edible oil production from microalgae: a review. Eur. J. Lipid Sci. Technol. 120, 1700428 https://doi.org/10.1002/ejlt.201700428.

Yang, Z.-K., Niu, Y.-F., Ma, Y.-H., Xue, J., Zhang, M.-H., Yang, W.-D., Liu, J.-S., Lu, S.-H., Guan, Y., Li, H.-Y., 2013. Molecular and cellular mechanisms of neutral lipid accumulation in diatom following nitrogen deprivation. Biotechnol. Biofuels 6, 67. https://doi.org/10.1186/1754-6834-6-67.